

AD

MEMORANDUM REPORT BRL-MR-3646

**AN INTERFEROMETRIC MEASUREMENT
TECHNIQUE FOR RAILGUN STRUCTURES**

**ALEX ZIELINSKI
JEFFREY KEZERIAN
MAJ. JOSEPH BENO**

JANUARY 1988

APPROVED FOR PUBLIC RELEASE, DISTRIBUTION UNLIMITED

**US ARMY BALLISTIC RESEARCH LABORATORY
ABERDEEN PROVING GROUND, MARYLAND**

UNCLASSIFIED
SECURITY CLASSIFICATION OF THIS PAGE

REPORT DOCUMENTATION PAGE

Form Approved
OMB No. 0704-0188

1a. REPORT SECURITY CLASSIFICATION Unclassified		1b. RESTRICTIVE MARKINGS	
2a. SECURITY CLASSIFICATION AUTHORITY N/A		3. DISTRIBUTION / AVAILABILITY OF REPORT	
2b. DECLASSIFICATION / DOWNGRADING SCHEDULE N/A			
4. PERFORMING ORGANIZATION REPORT NUMBER(S) BRL-MR-3646		5. MONITORING ORGANIZATION REPORT NUMBER(S)	
6a. NAME OF PERFORMING ORGANIZATION US Army Ballistic Research Laboratory	6b. OFFICE SYMBOL (if applicable) SLCBR-TB	7a. NAME OF MONITORING ORGANIZATION	
6c. ADDRESS (City, State, and ZIP Code) Aberdeen Proving Ground, Maryland 21005-5066		7b. ADDRESS (City, State, and ZIP Code)	
8a. NAME OF FUNDING / SPONSORING ORGANIZATION US Army Ballistic Research Laboratory	8b. OFFICE SYMBOL (if applicable) SLCBR-D	9. PROCUREMENT INSTRUMENT IDENTIFICATION NUMBER	
8c. ADDRESS (City, State, and ZIP Code) Aberdeen Proving Ground, Maryland 21005-5066		10. SOURCE OF FUNDING NUMBERS	
		PROGRAM ELEMENT NO 62618A	PROJECT NO AH80
		TASK NO. 00	WORK UNIT ACCESSION NO.
11. TITLE (Include Security Classification) (U) An Interferometric Measurement Technique for Railgun Structures			
12. PERSONAL AUTHOR(S) Alexander Zielinski, Jeffrey Kezerian, and Maj. Joseph Beno			
13a. TYPE OF REPORT MR	13b. TIME COVERED FROM _____ TO _____	14. DATE OF REPORT (Year, Month, Day)	15. PAGE COUNT
16. SUPPLEMENTARY NOTATION			
17. COSATI CODES		18. SUBJECT TERMS (Continue on reverse if necessary and identify by block number)	
FIELD	GROUP	Interferometry Railgun	
20	03	Bore expansion Magnetic Pressure	
		Pulsed Power Electric Gun	
19. ABSTRACT (Continue on reverse if necessary and identify by block number) A technique to measure the expansion of a railgun under conditions of high magnetic stress has been developed. Bore deflections are detected by a Michelson interferometer arrangement during the application of a current pulse which produced repulsive forces similar to those in an actual projectile launch. This technique has been successfully used with two different barrel set-ups whose rails were electrically connected outside the bore at the muzzle. The method should prove valuable for testing a wide variety of electromagnetic launcher structures owing to the small loading of the oprics on the structure itself.			
20. DISTRIBUTION / AVAILABILITY OF ABSTRACT <input checked="" type="checkbox"/> UNCLASSIFIED/UNLIMITED <input checked="" type="checkbox"/> SAME AS RPT <input type="checkbox"/> DTIC USERS		21. ABSTRACT SECURITY CLASSIFICATION UNCLASSIFIED	
22a. NAME OF RESPONSIBLE INDIVIDUAL Alex Zielinski		22b. TELEPHONE (Include Area Code) 301/278-5687	22c. OFFICE SYMBOL SLCBR-TB-EP

ACKNOWLEDGEMENT

The experimental work was performed while the authors were at Picatinny Arsenal, ARDEC, Dover, NJ.

TABLE OF CONTENTS

	Page
ACKNOWLEDGEMENT.....	iii
LIST OF FIGURES.....	vii
I. INTRODUCTION.....	1
II. INTERFEROMETER ARRANGEMENT.....	4
III. EXPERIMENT: MECHANICAL and ELECTRICAL.....	4
IV. OPTICAL and MECHANICAL CONSIDERATIONS.....	8
V. RESULTS.....	9
VI. CONCLUSIONS.....	14
REFERENCES.....	17
DISTRIBUTION LIST.....	19

LIST OF FIGURES

Figure	Page
1. Essential Features of an Electromagnetic Railgun.....	2
2. Interferometric Arrangement for Measurement of Rail Displacement...	3
3. Illustration of an Interference Fringe Pattern	5
4. Detailed Geometric Diagram for the Object Beam Path Length.....	6
5. Component Placement and Equivalent Circuit Schematic for the Table Top Experiment.....	7
6. Fringe Detector Output (upper plot) and Waveform Expansion for the First 800 Microseconds (lower plot) for the Table Top Experiment...	10
7. Typical Current Trace (upper curve) and Bore Expansion (lower curve) for the Table Top Experiment.....	11
8. Peak Bore Expansion versus Peak Current for the Table Top Experiments.....	12
9. Fringe Detector Output versus Time for the Short Barrel Section. Initial Capacitor Voltage = 2500 volts, and Peak Barrel Current = 314,000 amperes.....	13
10. Barrel Currents (upper plot) and Bore Expansions (lower plot) versus Time for Two Pulse Tests.....	15

I. INTRODUCTION

In a system designed to convert stored electrical energy to the energy of mechanical motion one is likely to produce large forces on the structure in addition to the desired forces. The problem of deflections of current carrying conductors and their effects on busbar supports has been studied in the power utility industry,¹ and more recently, in the development of electromagnetic launchers.^{2,3,4} The problem with busbars in the utility industry is aggravated by their having natural frequencies of a few hundred hertz so that mechanical resonance may be possible. During operation, electromagnetic launchers must cope with even higher transient currents than the utility industry must contend with under short circuit fault conditions. With the anticipated use of sequential pulsers (eg., Compulsators or other pulsed power supplies designed for high rate of fire) the EM gun community may also have to contend with resonance. In any of these cases, the failure of support structures resulting from transient magnetic forces can lead to degraded performance or catastrophic failure. A study of the structural behavior of a mechanical system can assist in preventing failure and optimizing the design for a given performance. In developing railguns as efficient, long life devices, an understanding of material deformation under pulse loading is necessary. The bore's dimensional integrity is important for both the armature and the projectile as they travel the length of the rail pair. Deformations may affect not only in bore conditions such as friction, balloting, and launch attitude, but also armature function; the fit of the armature to the bore is critical since the armature must complete the rail to rail circuit by maintaining two high current, sliding, electrical contacts.

The railgun type of electromagnetic launcher has been widely studied. The essential features of the railgun are shown in Fig. 1. In the simplest form of the device, current is applied to a normally stationary, parallel pair of conducting rails. A conductor, either solid or gaseous, free to slide between the rail pair, completes the circuit and also carries the same current. The moving conducting element is called the armature. The interaction between the current and its magnetic field produces a force tending to expand the current carrying loop; this leads, of course, to acceleration of the armature. Unfortunately, the same interaction which produces projectile acceleration also produces a transient, bore-distorting, repulsive force between the rails.

Interferometry is a technique which can be used to measure change in displacement of an object. Figure 2 is a schematic of a simple laser interferometer which shows the process of splitting a beam of coherent, monochromatic light into two beams. Beam A-D, the reference beam, never changes in length; beam A-B-C, the object beam, is reflected by the objects that will be moving. Both beams are reflected back on themselves and recombine at the splitter. This phase difference with different path lengths produces either constructive or destructive interference of the beams. As the path length of the object beam changes the alternatively constructive and destructive interference produces a sequence of light and dark fringes. Since the fringes result from phase difference in light of known wavelength a relationship between the number of fringes and movement of the object may be determined. In dynamic tests, an oscilloscope records the time-varying output of a simple photodetector which senses the varying light intensity as fringes are produced. From this record the actual change in rail separation versus time may be determined.

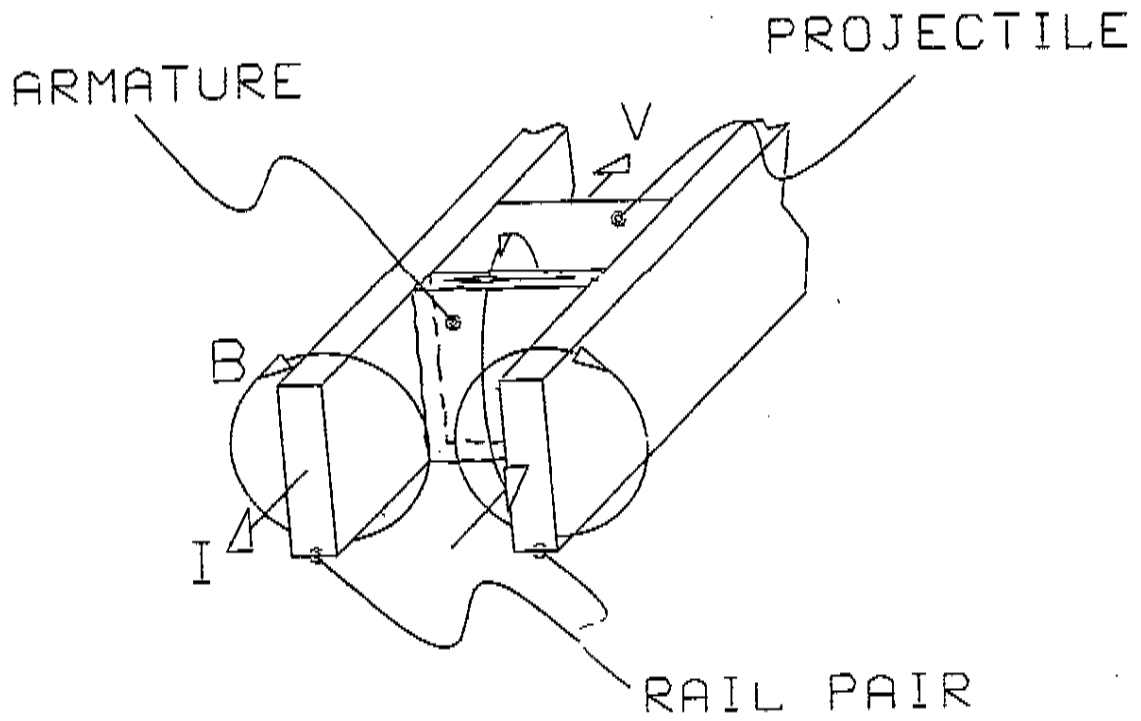


Figure 1. Essential Features of an Electromagnetic Railgun.

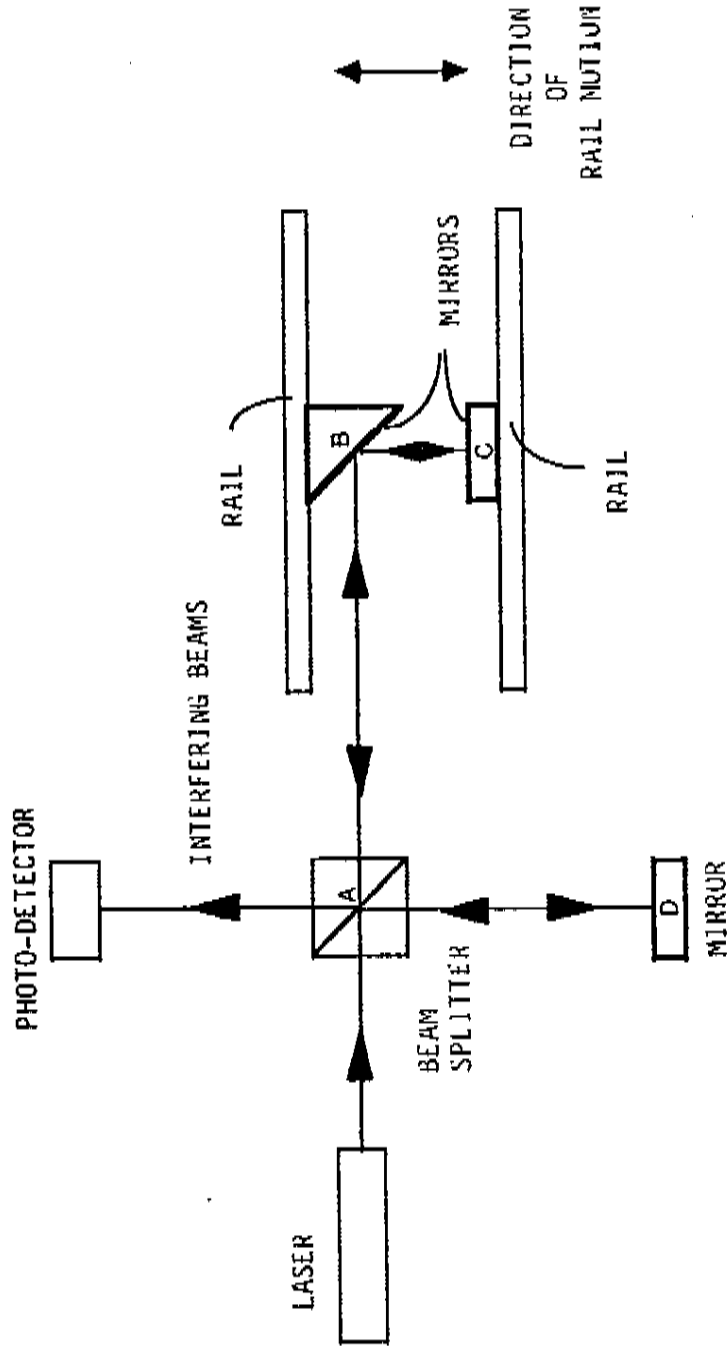


Figure 2. Interferometric Arrangement for Measurement of Rail Displacement.

In the work reported here, two sets of experiments were performed. The first consisted of a pair of rudimentary conducting fixed parallel aluminum beams, pulsed with currents less than 5,000 amperes, and the second was a short electromagnetic railgun barrel section designed for a peak pressure of 1.0 GPa (145 ksi) and pulsed with currents greater than 100,000 amperes.

II. INTERFEROMETER ARRANGEMENT

The interferometric components and their arrangement employed in both the table top experiments (aluminum beams) and the short barrel experiments are shown in Fig. 2. The laser light is divided by the beam splitter into reference and object paths. The path A-B-C-B-A changes length as the rails separate, the path A-D-A remains fixed. As mirrors B and C move apart, the interference pattern shifts at the detector. A path length change in A-B-C-B-A of one wavelength moves the fringe pattern by a given distance across the detector. An interference pattern of light and dark fringes is created similar to that shown in Fig. 3.

To determine how many fringes pass in front of the detector for a given change in rail pair separation let us assume that each mirror moves a distance of $\delta/2$, refer to Fig. 4. The original optical path is A-B₁-C₁-B₁-A and the displaced path is A-B₂-C₂-B₂-A. It can be seen that the total displaced path A-B₂-C₂-B₂-A is longer than the original path A-B₁-C₁-B₁-A by an amount equal to 2δ . The number of fringes passing the detector is $2\delta/\lambda$, where λ is the laser wavelength. Therefore the number of voltage waveform cycles per unit time on the oscilloscope is proportional to the rail pair separation change per unit time and is given by:

$$\delta(t) = N(t) * \lambda/2$$

where $N(t)$ is the number of detected peaks occurring in unit time.

III. EXPERIMENT: MECHANICAL AND ELECTRICAL

The table top experimental set-up and circuit used to provide power are shown schematically in Fig. 5. The aluminum rails are 2.286 mm (0.09 inch) thick, 146 mm (5.75 inches) long and 38.1 mm (1.5 inches) high with a nominal rail-to-rail separation distance of 25.4 mm (1 inch). Only the breech and muzzle ends of the rails are anchored to fiberglass/epoxy laminate (G-11) supports. At the breech a 5/8-inch bolt into a copper block is used to connect the current leads (12 gage wire) to the rails. Since no projectiles were used, the rails were shorted at the muzzle using two 3/8-inch steel bolts. The mirror, C, is mounted to one rail with double sided tape while the other mirror, B, is held at a 45 degree angle by a plexiglass mount attached to the other rail in the same manner. Both mirrors were located at the axial and transverse center of the rails.

The pulsing circuit for the table top experiment was designed to provide a current rise time of 120 microseconds which was expected for the short barrel experiments. The required total inductance for the table top pulser

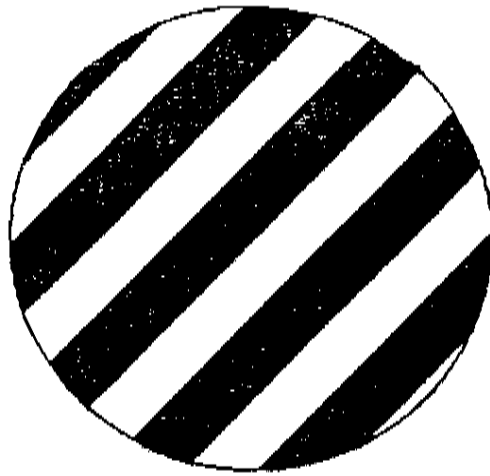


Figure 3. Illustration of an Interference Fringe Pattern.

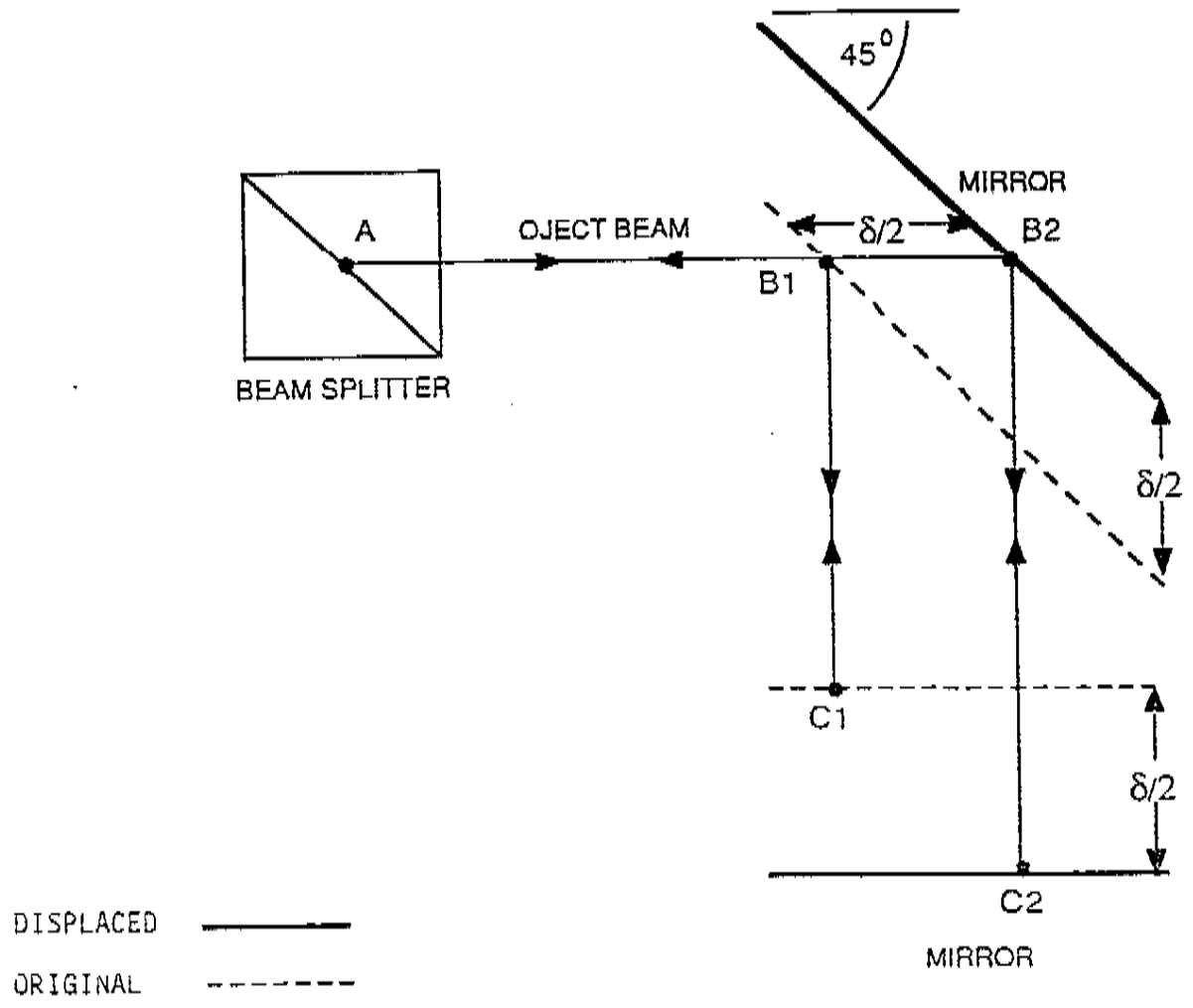


Figure 4. Detailed Geometric Diagram for the Object Beam Path Length.

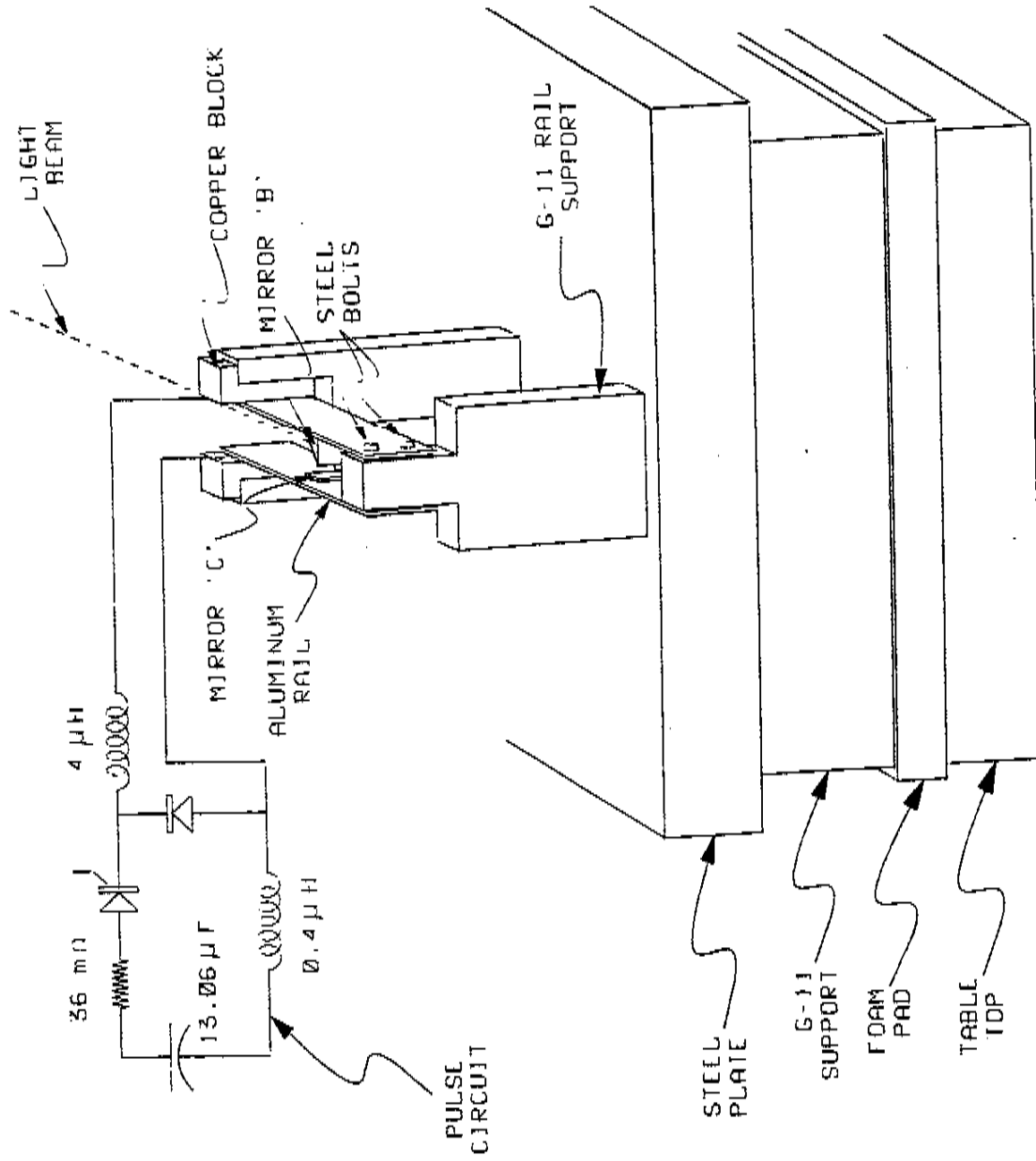


Figure 5. Component Placement and Equivalent Circuit Schematic for the Table Top Experiment.

was calculated to be:

$$L_{tot} = 4 * t_{pk}^2 / \pi^2 * Cap$$

where t_{pk} is the time for current to reach peak and Cap is the pulser capacitance. This yields an inductance of 4.4 microhenries. Most of this inductance (4.0 microhenries) has to be provided by an inductor in the form of a single layer solenoid. Using 12 gage wire and a 4-inch diameter form, the required number of turns to obtain an inductance of 4 microhenries is found from:⁵

$$N = [L * (9a + 10b)]^{1/2} / a$$

where, L is the inductance in microhenries, a is the mean radius of the solenoid and b is the length of the solenoid in inches. The calculated maximum obtainable bank current (resistance included) with the bank fully charged is 4973 amperes. This translates to an applied load per unit rail length of 153 N/m (0.88 lb/in) to the rail surface. For this static beam analysis predicts a maximum bore deflection of 24 micrometers (0.94 mils) at maximum charge.

A Rogowski coil was used to measure the circuit di/dt . The coil has an output conversion factor of 15.9 amps/volt-microsecond. The optical fringe detector consisted of a RCA hybrid silicon photodiode with integral preamplifier module. The output of the circuit was fed into a capacitive AC coupler with a 50-ohm terminator. The data was collected using a Nicolet 2090 oscilloscope.

For the short barrel experiments a different power source was used and is described elsewhere.^{6,7} Also, the mirrors were mounted in the bore and attached to the rails with epoxy. The interferometer was set up much the same way as for the table top experiment. The available current for these tests was greater than 100,000 amperes. Since the system energy was larger than in the table top experiments much more rigid optical supports were needed to control vibrations.

IV. OPTICAL AND MECHANICAL CONSIDERATIONS

The optical equipment was set up with several considerations in mind. First, the optical path differences must be within the coherence length of the laser. Since this length was unknown, any problem was circumvented by making the path lengths nearly equal.

A second consideration was the system's sensitivity. Because the interferometer will measure displacements smaller than an optical wavelength, extremely small vibrations result in fringes passing the detector. To avoid these small vibrations the apparatus was assembled on a massive board isolated by mounts of low stiffness. Thus, only low amplitude, low frequency vibrations were transferred to the equipment. The movement of the rails during a

current pulse produced temporal changes in the interference pattern which are significantly higher in frequency than those produced by external vibrations within the test area.

To avoid unwanted interference patterns that occur when the beam is reflected back on itself at the unsilvered interfaces of the beam splitter, the splitter was tilted slightly requiring mirror "D" to be moved for compensation. Now the two paths A-D and A-B in Fig. 2 become non-perpendicular and secondary interference patterns do not appear where the detector is located. Secondary reflections at the flat mirrors were eliminated by the use of front-surface silvered mirrors.

In the short barrel, high current experiments the two rail mirrors were unintentionally misaligned slightly and this resulted in the incoming beam, A-B being off axis with the return beam, B-A. This was compensated by adjustment of the trajectory of the incoming beam. Also, the reference beam optics were mounted on a 1 inch thick, G-11 platform bolted to the muzzle end of the barrel. A fiber optic cable transmitted the interference pattern to the detector a few meters away.

The above considerations were generally easy to compensate for and did not significantly hinder the experiment once the initial set-up was refined.

V. RESULTS

In the table top experiment the capacitor bank current was limited to less than 5000 amperes. There was no containment structure to keep the aluminum rail pair from deflecting. In this configuration it was found that measurable deflections occurred even with low currents. The short barrel section structure was designed for a peak pressure of 1.0 GPa (145 ksi) and therefore currents greater than 100,000 amperes were needed to produce detectable bore deflections.

Five tests were performed on the table top experiment at different bank energies. For each energy similar waveforms were observed. A typical detector waveform output recorded on a Nicolet 2090 oscilloscope is shown in Fig. 6a. The expansion of this waveform for the first 800 microseconds is shown in Fig. 6b. In the first 800 microseconds 43 fringes moved across the detector. The velocity of the rails is directly related to the instantaneous frequency of the output signal. Maximum velocity was reached near 300 microseconds. The aluminum rails used in the table top experiment exhibited a slightly damped oscillatory motion from a single current pulse. One complete cycle of mechanical oscillation was observed to have a frequency of 280 hertz. The current and deflection curves versus time for one test are plotted in Fig. 7. Figure 8 is a summary plot of peak current (at 115 microseconds) versus peak bore deflection (at 728 microseconds) for the five small scale tests. The bore deflections scale as the square of the current.

Two tests were performed on the short barrel section: one where 110,000 amperes was delivered to the barrel section (capacitor voltage = 1000 volts), and one where 314,000 amperes was produced (capacitor voltage = 2500 volts). Shown in Fig. 9 is the optical fringe detector output for the higher current test. This total trace is comprised of five separate waveforms, each recorded

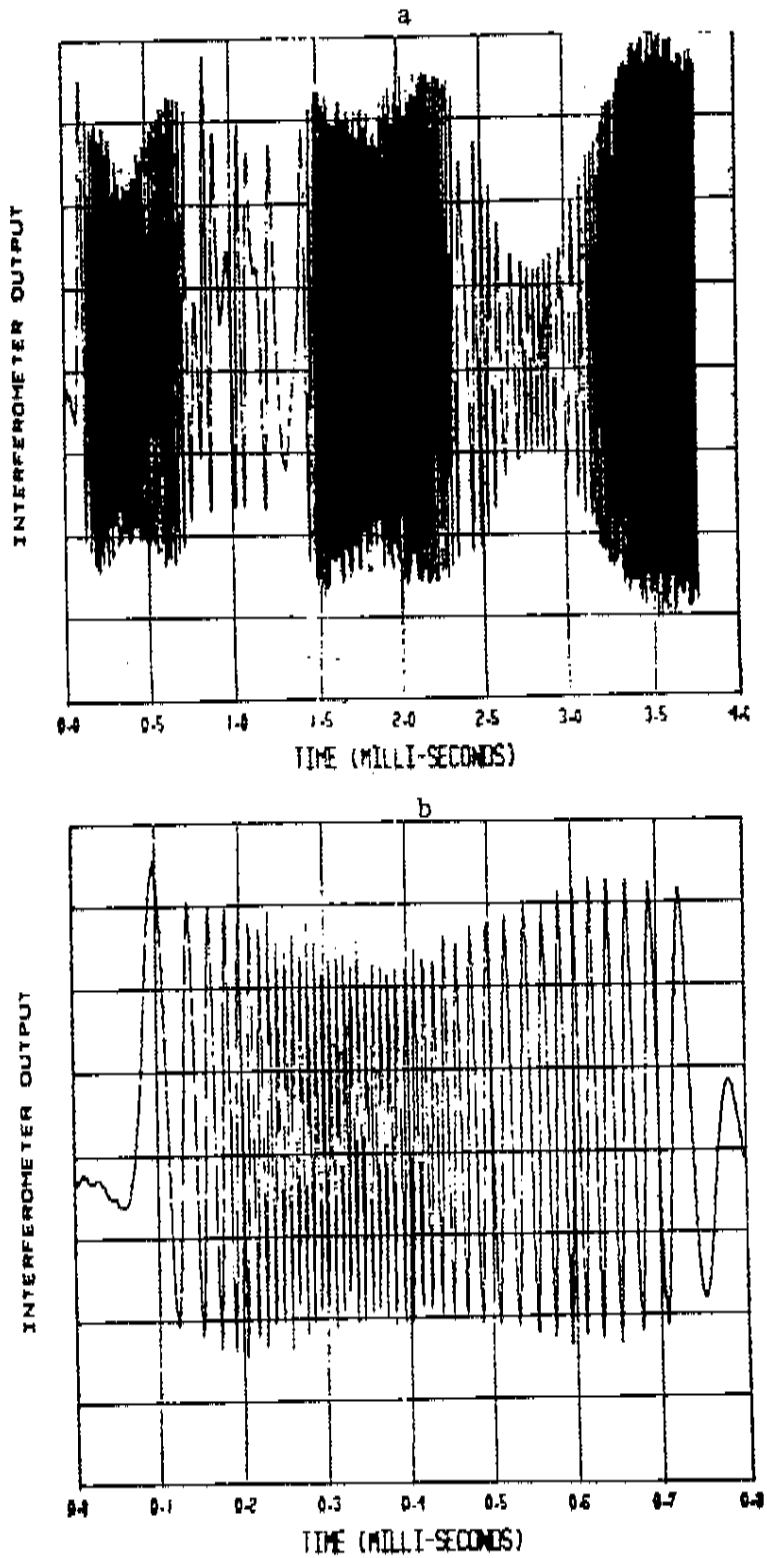


Figure 6. Fringe Detector Output (upper plot) and Waveform Expansion for the First 800 Microseconds (lower plot) for the Table Top Experiment.

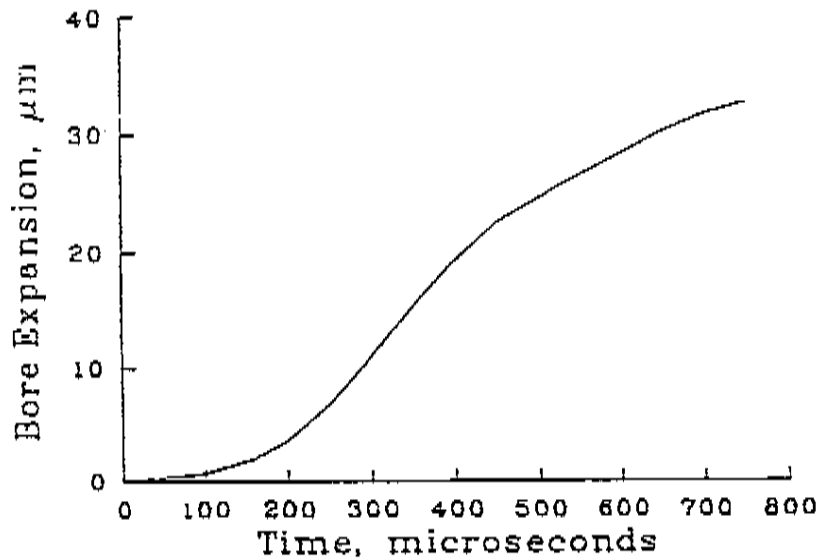
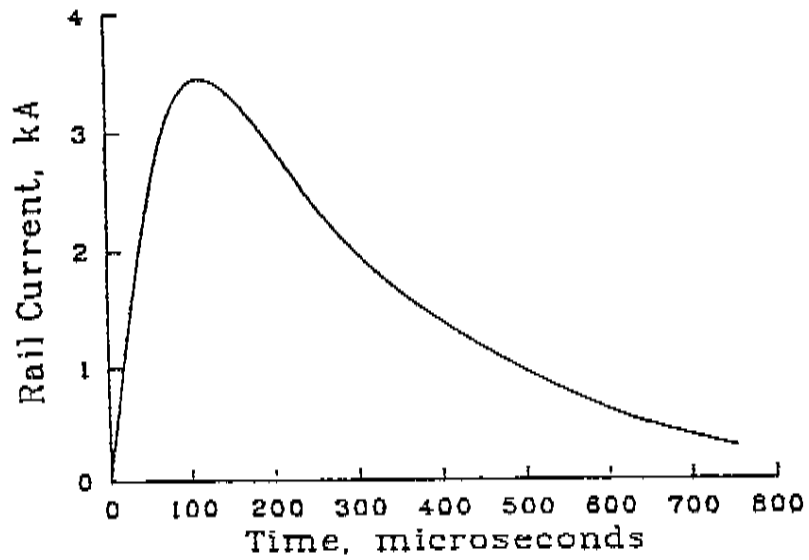


Figure 7. Typical Current Trace (upper curve) and Bore Expansion (lower curve) for the Table Top Experiment.

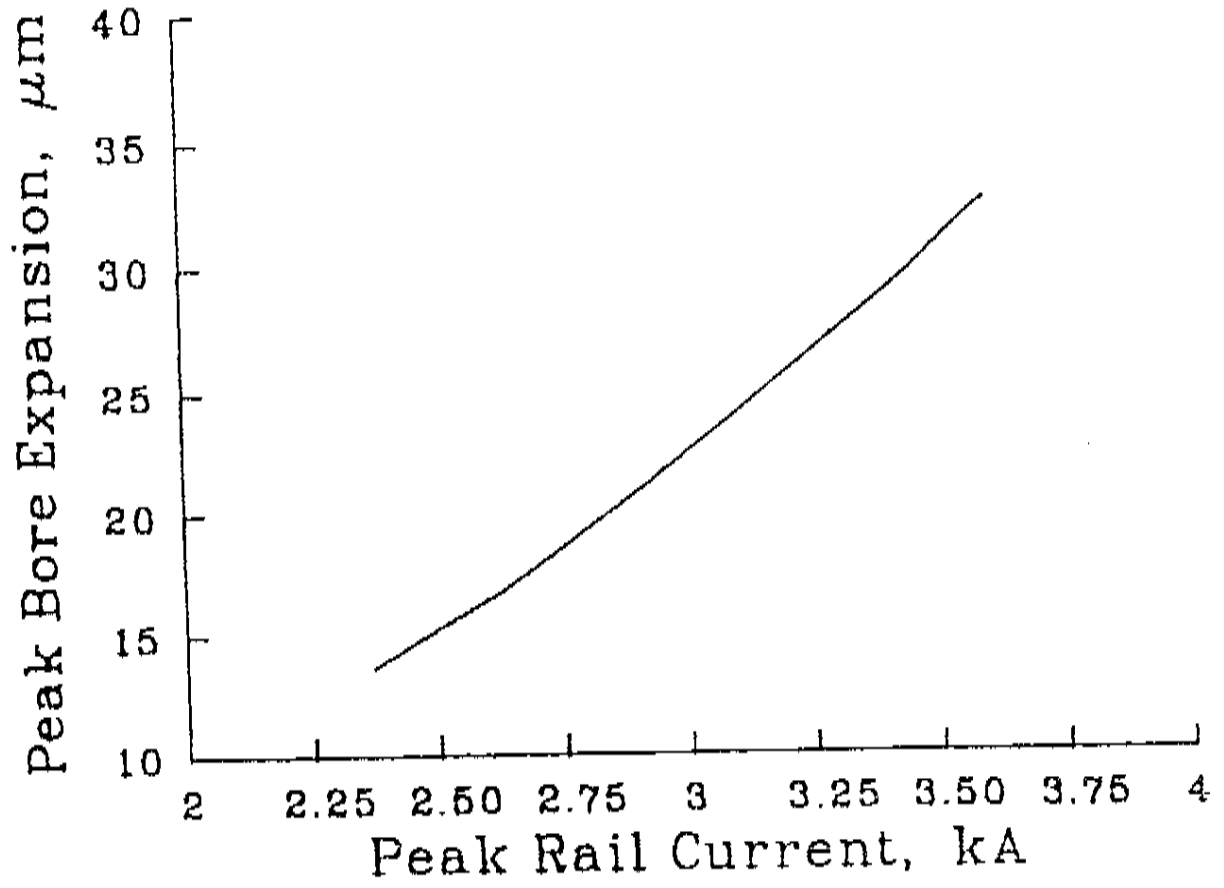


Figure 8. Peak Bore Expansion versus Peak Current for the Table Top Experiments.

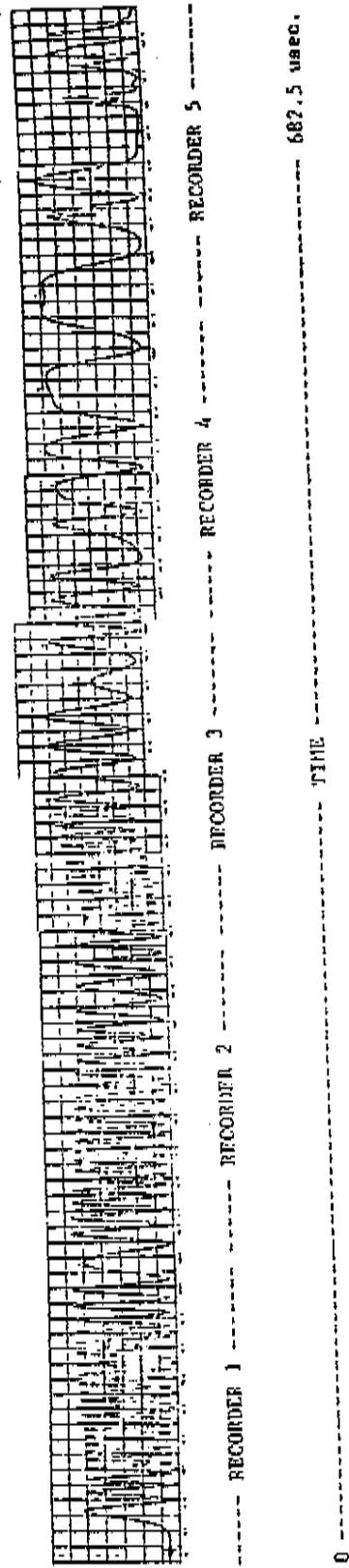


Figure 9. Fringe Detector output versus Time for the Short Barrel Section. Initial Capacitor Voltage = 2500 volts, and Peak Barrel Current = 314,000 amperes.

on a Tektronix 390 AD transient digitizer operated in the serial mode. The reduced fringe detector signal amplitude concurrent with the lower signal frequency is representative of peak deflection and approximately zero rail velocity. This condition occurred twice; on the 24th fringe (131.5 microseconds) and on the 65th fringe (380.5 microseconds). After the 74th fringe (604 microseconds) rail movement has stopped and only background vibrations are sensed by the detector. A plot of the bore expansion versus time for both the low and high current tests, are shown in the bottom portion of Fig. 10. The peak current (upper portion of Fig. 10) occurred at 112 microseconds while the maximum bore deflection occurred between 117 and 143 microseconds.

In the table top experiment the aluminum rails have moved less than 10% of their peak deflection at peak current where as the short barrel-section rails have moved 95% of their final deflection at peak current. Maximum current in the table top experiment was 3600 amperes, and was 314,000 amperes in the short barrel tests. The corresponding bore expansions obtained were 32.5 micrometers ($1.28E-3$ inches) and 7.6 micrometers ($0.298E-3$ inches), respectively.

VI. CONCLUSION

The laser interferometric technique has proven useful in making small, dynamic deflection measurements in systems under large electrical and mechanical stress. The interference signal pattern was easily transmitted to the detector a few meters away via a fiber optic cable. Two drawbacks to this technique become evident when recording and analyzing the data. First, for large deflections a trade-off has to be made between the sampling rate and the window width of the oscilloscope. Second, with this technique the interferometer measures separation change without indicating whether the rails have, expanded, contracted, or translated together. This can produce some ambiguity in the data reduction if the initial direction of rail motion is not known. The maximum separation occurs when the waveform becomes reduced in both frequency and amplitude. When no rail motion is occurring only system vibrations are observed by the detector and these appear as slight noise in the signal. The needed accuracy in these experiments does not require the use of expensive optical components although access to the proper equipment greatly facilitated the set-up and alignment of the interferometer. The technique allows immediate return of the data and excellent measurement accuracy.

With electromagnetic gun developers requiring much stiffer railgun barrels this technique should provide a valuable tool for structural diagnostics and verification of finite element analysis.

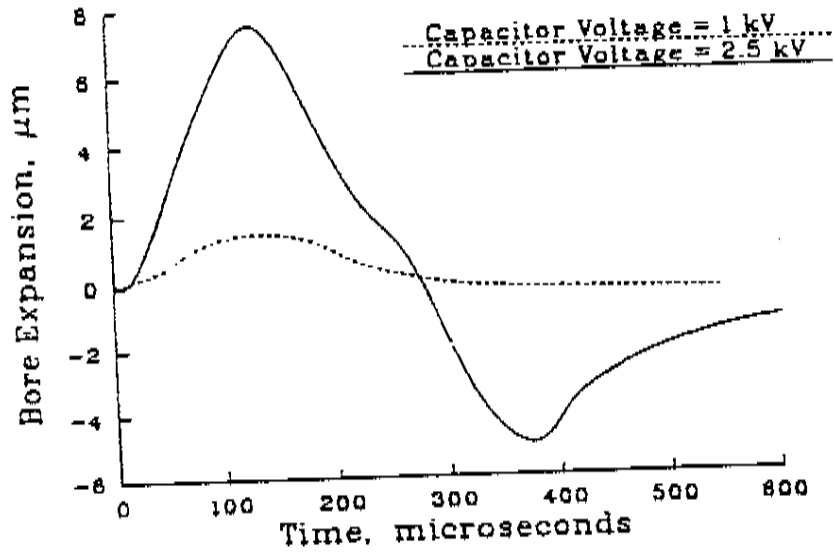
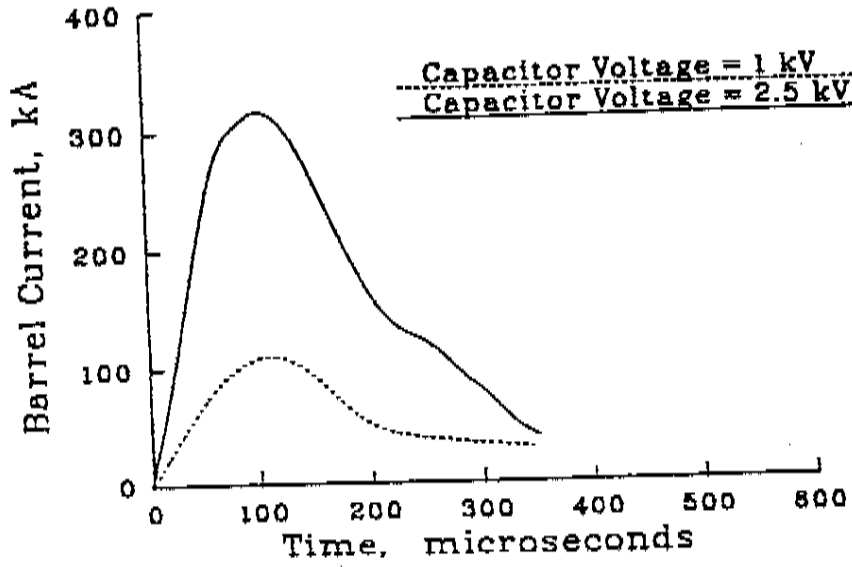


Figure 10. Barrel Currents (upper plot) and Bore Expansions (lower plot) versus Time for Two Pulse Tests.

REFERENCES

1. Schuring, O. R., and Sayre, M. F., "Mechanical Stresses in Busbar Supports During Short Circuits", Journal of American Institute of Electrical Engineers, pp. 44, 1925
2. Zimmerman, E. L., Fowler, C. M., Foley, E., and Parker, J. V., "HIMASS Electromagnetic Launcher at Los Alamos," IEEE Transactions on Magnetics, Vol. Mag-22, pp. 1823-1825, Nov 1986.
3. Davidson, R. F., Cook, W. A., Rabern, D. A., and Schnurr, N. M., "Predicting Bore Deformations and Launcher Stresss in Railguns," IEEE Transactions on Magnetics, Vol. Mag-22, pp. 1435-1440, Nov 1986.
4. Wang, S. Y., "Structural Response of a Rail Accelerator," IEEE Transactions on Magnetics, Vol. Mag-22, pp. 356-359, March 1984.
5. Terman, F., Radio Engineers' Handbook, McGraw-Hill Book Company, Inc., New York, NY, 1943.
6. Zielinski, A., Jamison, K., and Bennett, J., Pulse Current Transformer for Low Inductive Loads, BRL-MR-3626, Ballistic Research Laboratory, Aberdeen Proving Ground, MD, Oct, 1987.
7. Pappas, J., Driga, M. D., and Weldon, W., High Current Coaxial Pulse Transformer for Railgun Applications, Paper presented at the 5th IEEE Pulsed Power Conference, Arlington, VA, June, 1985.